TPIMx (x = 0, 6)
TPIM0: R' = H,
TPIM6: R' = C$_6$H$_{13}$

➤ **Imidazole is found in bioactive compounds.**

➤ **Proton donor as well as acceptor.**

➤ **Expansion of triphenylene ring=>Extension of aromatic ring=>mesomorphic over broad temperature ranges and exhibit high charge carrier mobilities**

6TPIM0

6TPIm0

6TPIm6

Off 6TPIMF
On 6TPIMF
Off (6TPIMF+Au)
On (6TPIMF+Au)
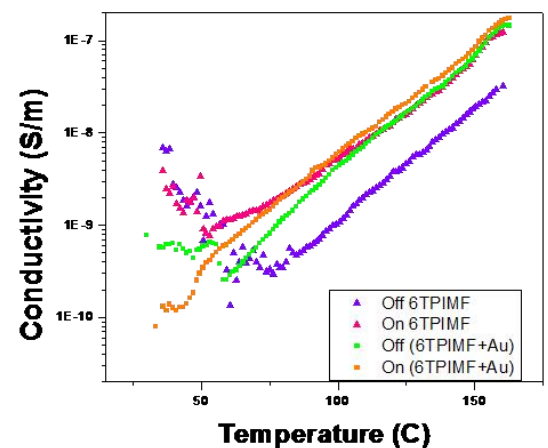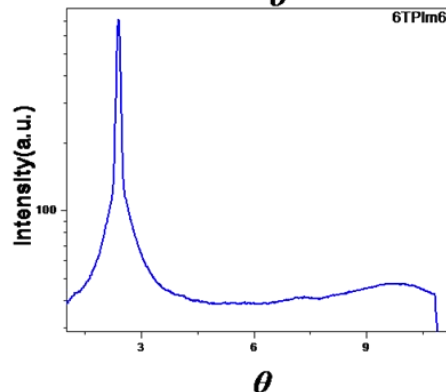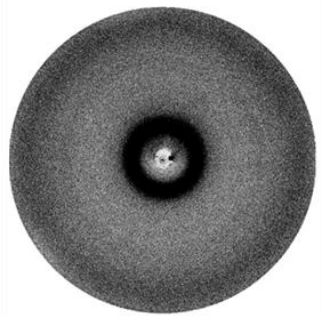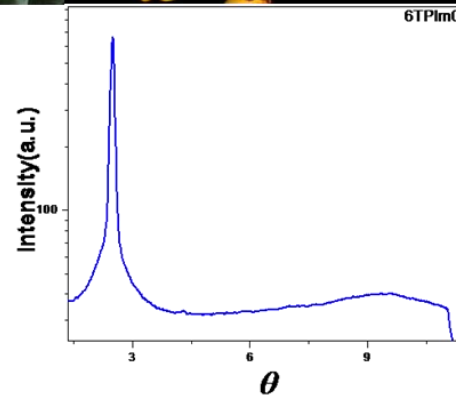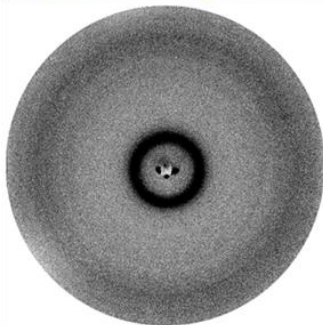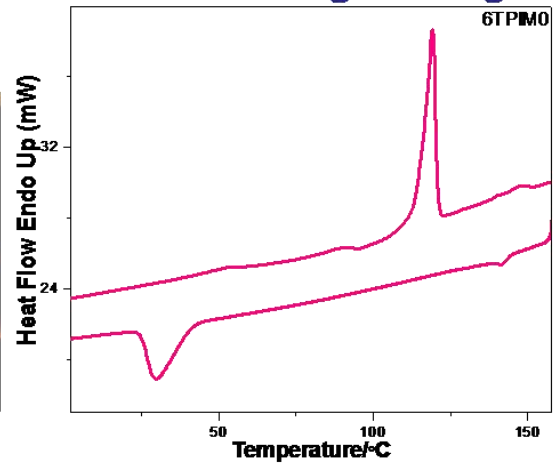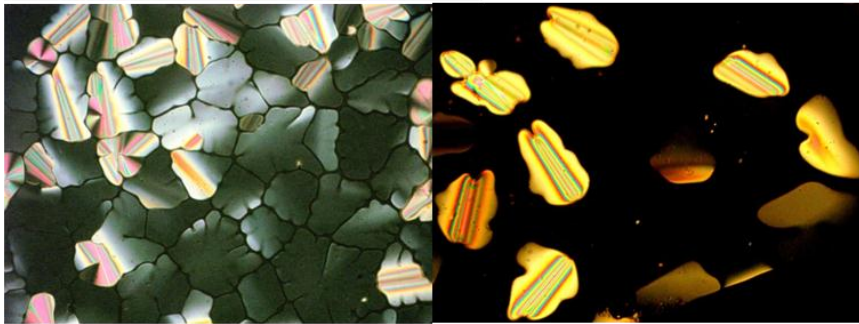
5.1. Introduction

One of the largest and most important classes of molecules that exhibit columnar liquid crystal phases is represented by triphenylene derivatives. Triphenylenes are, to date, the most widely explored materials out of all discotic mesogens since the triphenylene core is easily accessible through recognized synthetic routes, and is excellent at granting mesomorphic properties.[1] Research over the past decade has plentifully demonstrated the potential that these and related materials have as components in semiconductor devices such as LEDs, solar cells, field effect transisters etc.[2] Hexasubstituted triphenylene derivatives (Ester and Ether) are the most broadly examined discotic materials because they have a strong tendency to form columnar mesophases, which are of interest for one-dimensional energy and electron transport, and they have also been exploited in optical compensation films in optoelectronic devices.[3] Structure–property relationships of triphenylene-based discotic mesomorphic materials have been fully explored because of their considerable technological importance.

Molecular shape is one of the most imperative factors which determines the self-assembly of molecules into mesomorphic phases. Expansion of triphenylene ring is expected to lead to dramatic changes in phase behavior, since the extension of aromatic ring would, in effect, give rise to a mesogen with a core that is both much larger and of a different shape. These supramolecular macro discotics are anticipated to be mesomorphic over broad temperature ranges[4] and exhibit high charge carrier mobilities[5] in their columnar phases.

[1] S. Kumar, *Liq. Cryst.,* 31, 1037, **2004**.

[2] Boden, N.; Movaghar, B. In *Handbook of Liquid Crystals;* D. Demus, J. Goodby, G. W. Gray, H. -W. Spiess, V. Vill, Eds., Wiley-VCH: New York, Vol. 2b, pp. 781, **1998**.

[3] (a) K. Kawata, *Chem. Rec.,* 2, 59, **2002**; (b) S. Kumar, P. Schuhmacher, P. Henderson, J. Rego, H. Ringsdorf, *Mol. Cryst. Liq. Cryst. A,* 288, 211, **1996**; (c) N. Boden, R. J. Bushby, J. Clements, B. J. Movaghar, *J. Mater. Chem.,* 9, 2081, **1999**.

[4] (a) A. M. van de Craats, J. M. Warman, K. Mullen, Y. Geerts, J. D. Brand, *Adv. Mater.,* 10, 36, **1998**; (b) G. R. J. Muller, C. Meiners, V. Enkelmann, Y. Geerts, K. Mullen, *J. Mater. Chem.,* 8, 61, **1998**; (c) K. Msayib, S. Mahkseed, N. B. McKeown, *J. Mater. Chem.,* 11, 2784, **2001**; (d) P. Herwig, C. W. Kayser, K. Mullen, H.-W.

Triphenylene derivatives with six alkoxy chains are liquid crystalline, triphenylenes having less than six alkoxy chains are nonmesomorphic, but can be made mesomorphic by putting other substituents in the periphery.[3b,6] The concept of reducing symmetry is adopted by several workers with the basic idea that if the molecular symmetry is reduced, then the molecules would pack less favourably in the crystal state and, therefore, the melting point will decrease. The symmetry of a discoid molecule can be reduced by different ways, such as core asymmetric substitution, for example, putting 5 or 7 peripheral chains in a triphenylene molecule, or side chains asymmetry by attaching alkyl chains of different length in the periphery or by changing the mode of the attachment of the peripheral chains e. g. mixed ether-ester derivatives.

Imidazole skeleton is an integral part of numerous bioactive compounds which are known for their antiviral, anti-ulcer, anti-hypertension and anticancer properties.[7] Biological activity of imidazole derivatives is the main reason for their application in agriculture, medicine and pharmaceutical industry.[8] Additionally, the materials based on imidazole also have a great prospective in the area of fuel cell membranes,[9] ion-conducting electrolytes,[10] optical and chemical sensors,[11] luminescent materials[12] and photovoltaic materials for solar

Spiess, *Adv. Mater.*, 8, 510, **1996**; (e)C.-Y. Liu, A. Fechtenkoetter, M. D. Watson, K. Muellen, A. J. Bard, *Chem. Mater.*, 15, 1, 124, **2003**; (f) T. Yatabe, M. A. Harbison, J. D. Brand, M. Wagner, K. Mullen, P. Samori, J. Rabe, *J. Mater. Chem.*, 10, 1519, **2000**; (g) A. N. Cammidge, H. Gopee, *Chem. Commun.*, 966, **2002**; (h) N. Boden, R. J. Bushby, G. Headdock, O. R. Lozman, A. Wood, *Liq. Cryst.*, 28, 139, **2001**.

[5] A. M. van de Craats, J. M. Warman, *Adv. Mater.*, 13, 130, **2001**.

[6] (a) P. Henderson, S. Kumar, J. A. Rego, H. Ringsdorf and P. Schuhmacher, *J. Chem. Soc., Chem. Commun.*, 1059, **1995**; (b) J. A. Rego, S. Kumar, H. Ringsdorf, *Chem.Mater.*, 8, 1402, **1996**; (c) J. A. Rego, S. Kumar, I. J. Dmochowski, H. Ringsdorf, *Chem. Commun.*, 1031, **1996**.

[7] L. Nagarapu, S. Apuri, S. Kantevari, *J. Mol. Catal. A: Chem.* 266, 104, **2007**.

[8] (a) A. F. Pozharskii, A. T. Soldatenkov, A. R. Katritzky, *Heterocycles in Life and Society*; John Wiley & Sons; Chichester, **1997**; (b) E. G. Brown, *Ring Nitrogen and Key Biomolecules*; Kluwer Academic: Dordrecht, **1998**.

[9] (a) M. Schuster, W. H. Meyer, G. Wegner, H. G. Herz, M. Ise, K. D. Kreuer, J. Maier, *Solid State Ionics*, 145, 85, **2001**; (b) W. Munch, K. -D. Kreuer, W. Silvestri, J. Maier, G. Seifert, *Solid State Ionics,* 145, 437, **2001**; (c) H. Pu, L. Qiao, *Macromol. Chem. Phys.*, 206, 263, **2005**.

[10] (a) M. Yoshio, T. Kagata, K. Hoshino, T. Mukai, H. Ohno, T. Kato, *J. Am. Chem. Soc.*, 128, 5570, **2006**; (b) K. Kishimoto, T. Suzawa, T. Yokota, T. Mukai, H. Ohno, T. Kato, *J. Am. Chem. Soc.*, 127, 15618, **2005**; (c) M. Yoshio, T. Mukai, H. Ohno, T. Kato, *J. Am. Chem. Soc.*, 126, 994, **2004**.

[11] (a) N. Fukuda, J. Y. Kim, T. Fukuda, H. Ushijima, K. Tomada, *Jpn. J. Appl. Phys.*, 45, 460, **2006**; (b) H. Chao, B. -H. Ye, Q. -L. Zhang, L. -N. Ji, *Inorg. Chem. Commun.*, 2, 338, **1999**.

[12] (a) H. -J. Knolker, R. Hitzemann, R. Boese, *Chem. Ber.*, 123, 327, **1990**; (b) L. Zhao, S. B. Li, G. A. Wen, B. Peng, W. Huang, *Mater. Chem. Phys.*, 100, 460, **2006**.

cell applications.[13] Imidazole moiety is also personalized for hydrogen bond formation.[14] Hydrogen bonding caused by imidazole ring plays an important role in the formation of supramolecular mesomorphic aggregates. Imidazole moiety functions both as proton donor as well as proton acceptor.[15] There have been reports of design and construction of supramolecular mesomorphic assembly on the basis of imidazole moiety.[16] Strong intermolecular hydrogen bonding resulted in formation of supramolecular bilayers of smectogens by the assembly of linear imidazole-containing Schiff's bases.[17] Kadkin et al. reported smectic mesomorphism in imidazole-based biforked amphiphiles.[18] The structure of smectic phase had bilayered structure with a continuous network of hydrogen bonds. Imidazole has also been used as ligand for complexation with metal to achieve metallomesogens.[17,19]

However, most of the liquid crystalline materials based on imidazole skeleton come from the category of ionic liquids (Chapter 3), the mesomorphic materials based on molecular imidazole derivatives have been less investigated. Imidazole based bis(imidazole)-annulated discotic terphenyl derivatives **1** have been reported by Pisula et al.[20] Columnar order with helical stacking of discs within the column was observed in these compounds. The compound **1b** with bulkier peripheral alkyl chains has lower isotropization temperature as compared to **1a**. These materials were thermally stable up to 350 °C. Very recently, the effect of extension of electron deficient π–conjugated perylene core has been investigated in perylene diester benzimidazole derivatives **2**. Wicklein et al. prepared a series of compounds **2a-c** in which

[13] M. Wang, X. Xiao, X. Zhou, X. Li, Y. Lin, *Sol. Energy Mater. Sol. Cells*, 91, 785, **2007**.

[14] (a) S. K. Amini, N. L. Hadipour, F. Elmi, *Chem. Phys. Lett.*, 391, 95, **2004**; (b) T. Ueda, S. Nagatomo, H. Masui, N. Z. Nakamura, *Naturforsch*, 54a, 437, **1999**; (c) Y. Wei, A. C. D. Dios, A. E. McDermott, *J. Am. Chem. Soc.*, 121, 10389, **1999**; (d) S. Nagatomo, S. Takeda, H. Tamura, N. Nakamura, *Bull. Chem. Soc. Jpn.*, 68, 2783, **1995**; (e) M. Torrent, D. G. Musaev, K. Morokuma, S. -C. Ke, K. Warncke, *J. Phys. Chem. B*, 103, 8618, **1999**.

[15] (a) M. T. Green, *J. Am. Chem. Soc.*, 122, 9495, **2000**; (b) A. Katrusiak, *J. Mol. Struct.*, 474, 125, **1999**; (c) H. R. Flakus, A. Bryk, *J. Mol. Struct.*, 372, 215, **1995**; (d) B. Brzezinski, G. Zundel, *J. Mol. Struct.*, 446, 199, **1998**.

[16] (a) T. Kato, T. Kawakami, *Chem. Lett.*, 211, **1997**; (b) A. Kraft, A. Reichert, R. Kleppinger, *Chem. Commun.*, 1015, **2000**; (c) S. H. Seo, J. H. Park, G. N. Tew, J. Y. Chang, *Soft Matter*, 2, 886, **2006**; (d) S. H. Seo, G. N. Tew, J. Y. Chang, *Tetrahedr. Lett.*, 48, 6839, **2007**.
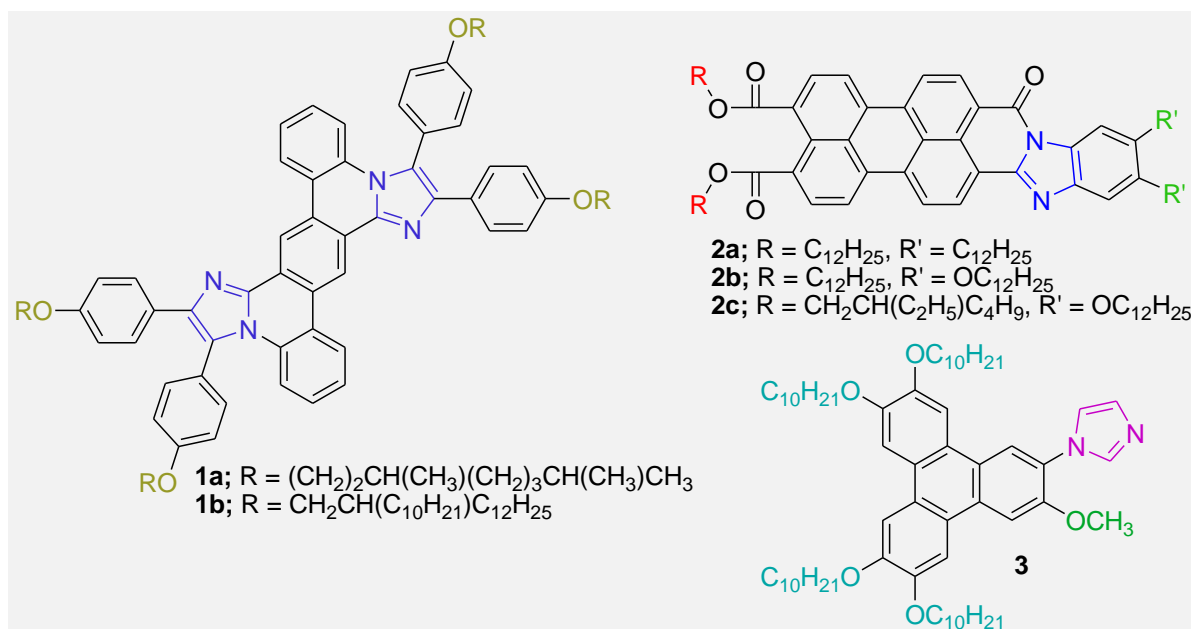
[17] O. N. Kadkin, J. Tae, E. H. Kim, S. Y. Kim, M. -G. Choi, *Supramol. Chem.*, 22, 1, 1, **2010**.

[18] O. N. Kadkina, J. Taea, S. Y. Kima, E. H. Kima, E. Leea, M. –G. Choi, *Liq. Cryst.*, 36, 12, 1337, **2009**.

[19] (a) F. –F. Jian, K. –F. Wang, *Liq. Cryst.*, 35, 12, 1415, **2008**; (b) S. J. Hsu, K. M. Hsu, M. K. Leonga, I. J. B. Lin, *Dalton Trans.*, 1924, **2008**; (c) W. Dobbs, J. M. Suisse, L. Douce, R. Welter, *Angew. Chem. Int. Ed.*, 45, 4179, **2006**.

[20] W. Pisula, F. Dierschke, K. Mullen, *J. Mater. Chem.*, 16, 4058, **2006**.

one side of perylene ring had diester and the anhydride ring of the second side was fused with benz-imidazole unit.[21]

1a; R = (CH₂)₂CH(CH₃)(CH₂)₃CH(CH₃)CH₃
1b; R = CH₂CH(C₁₀H₂₁)C₁₂H₂₅

2a; R = C₁₂H₂₅, R' = C₁₂H₂₅
2b; R = C₁₂H₂₅, R' = OC₁₂H₂₅
2c; R = CH₂CH(C₂H₅)C₄H₉, R' = OC₁₂H₂₅

3

All three derivatives displayed thermotropic hexagonal columnar mesophase. Liquid crystallinity was retained up to room temperature for derivatives **2b,c** having alkoxy chain in the benz-imidazole moiety. **2b** exhibited columnar plastic phase at lower temperature. Extension of π-conjugation due to fusion with benz-imidazole was confirmed by a red shift in absorption spectra as compared to perylene bisimide. Imidazole group has been connected via a single bond to tetraalkoxymonomethoxy triphenylene in the compound **3**.[22] In its pure form this compound was non-liquid crystalline, while a mixture of **3** with benzene-1,3,5-tricarboxylic acid in 1:3 molar ratio displayed mesomorphism over a broad thermal range. The hexagonal columnar structure of the mesophase was established by XRD study. On the basis of lattice constant values and the approximate diameter of single **3**, it was assumed that each disc of the column was constructed from arrangement of three molecules of **3**, connected to central benzene-1,3,5-tricarboxylic acid via hydrogen bonding. Also long range intracolumnar order was verified by the presence of a sharp peak in wide angle region.

---

[21] A. Wicklein, M. –A. Muth, M. Thelakkat, *J. Mater. Chem.*, 20, 8646, **2010**.
[22] M. Kimura, T. Hatanaka, H. Nomoto, J. Takizawa, T. Fukawa, Y. Tatewaki, H. Shirai, *Chem. Mater.*, 22, 5732, **2010**.

5.2. Objective

It is possible to have broad mesophase range as well as improved conductivity by appropriate balance between the size of rigid discotic core and peripheral insulating chains. In present investigation, we have looked over unsymmetrical examples of triphenylene-imidazole-fused derivatived for the effect of extention of discotic core on the mesomorphic behavior and charge carrier mobility in their liquid crystalline phase.

In this chapter, we report the extension of triphenylene ring with nitrogen containing heterocycle *i.e.* imidazole. We adopted this approach to increase π-electron conjugation as well as to reduce overall symmetry of triphenylene ring. We discuss the synthesis, characterization and mesomorphism of novel triphenylene-imidazole-fused mesogens. The number of peripheral alkyl chains around triphenylene have been varied between 5 and 6.

TPIMx (x = 0, 6)
TPIM0: R' = H,
TPIM6: R' = C$_6$H$_{13}$
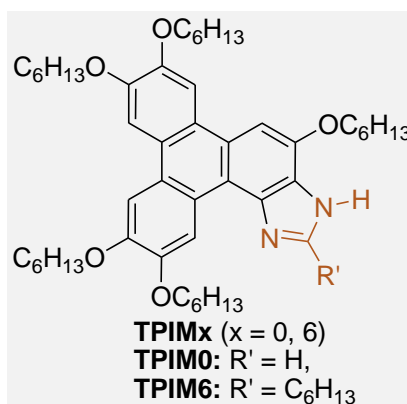
5.3. Synthesis

Synthesis starts from monohydroxytriphenylene **6TPOH** and goes via triphenylene-based o-quinone or 1,2-quinone **6TPCO2**. Monohydroxytriphenylene **6TPOH** was prepared starting from catechol as reported previously in chapter 2. *Ortho*-benzoquinone or 1,2-benzoquinone, an integral part of **6TPCO2**, is a precursor to many natural products. It is obtained either from ortho oxidation of a phenol or oxidation of catechol by exposing latter to

air in aqueous solution.[23] The oxidative dearomatization of phenols to achieve o-quinone or 1,2-quinone using various oxidising agents has been reported earlier.[24] These reagents include fremy's radical, o-iodoxybenzoic acid (IBX), hydrogen peroxide, ceric ammonium nitrate etc. Oxidation of the 2-hydroxy-3,6,7,10,11-pentakis(alkoxy)triphenylenes with a range of oxidising agents such as chromium trioxide, nitric acid and ceric ammonium nitrate resulted in the formation of o-quinone derivatives *i.e.* 3,6,7,10,11-pentakis(alkoxy)triphenylene-1,2-diones.[25] The synthesis of **6TPIMx** has been outlined in Scheme 1.
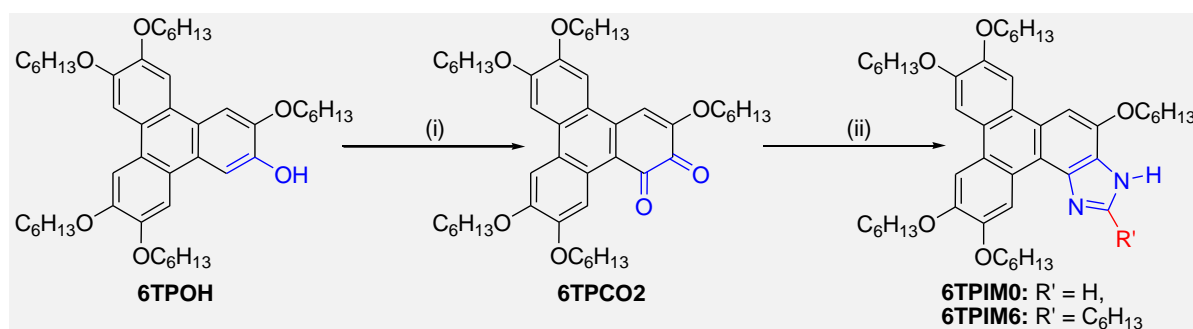
Scheme 1. Synthesis of triphenylene-imidazole-fused mesogens. (i) CAN, CH$_3$CN, rt, 2 min (yield = 65.33 %); (ii) R'CHO, CH$_3$COONH$_4$, CH$_3$COOH, refluxed, 5 hrs (yield = 26.69 %).

The first step of synthesis involves ceric ammonium nitrate mediated oxidation of monohydroxytriphenylene **6TPOH** to furnish 1, 2-diketone derivative **6TPCO2**. This was followed by coupling of 1, 2-diketone with ammonia and aldehyde in presence of acetic acid under reflux condition to produce the desired product.

5.4. Cheracterization

Both compounds were purified by repeated recrystallization and characterized from their ^{1}H NMR, UV spectra, MS and elemental analysis. Both compounds give similar spectra. Spectral data and elemental analysis of these compounds were in good agreement with their

[23] (a) D. Magdziak, A. A. Rodriguez, R. W. Van De Water, T. R. R. Pettus, *Org. Lett.*, 4, 2, 285, **2002**; (b) C. Parulekar, S. Mavinkurve, *Indian Journal of Experimental Biology,* 44, 157, **2006**.
[24] (a) H. Zimmer, D. C. Lankin, S. W. Horgan, *Chem. Rev.*, 71, 2, 229, **1971**; (b) C. Ran, D. Xu, Q. Dai, T. M. Penning, I. A. Blair, R. G. Harvey, *Tetrahedron Letters*, 49, 4531, **2008**; (c) A. Wu, Y. Duan, D. Xu, T. M. Penning, R. G. Harvey, Tetrahedron, 66, 2111, **2010**; (d) S. M. S. Chauhan, B. Kalra, P. P. Mohapatra, *Journal of Molecular Catalysis A: Chemical*, 137, 85, **1999**.
[25] S. Kumar, M. Manickam, S. K. Varshney, D. S. Shankar Rao, S. K. Prasad, *J. Mater. Chem.*, 10, 2483, **2000**.

structures, indicating the high purity of all the materials. Figure 1 represents the ^{1}H NMR spectrum of precursor **6TPCO2**.
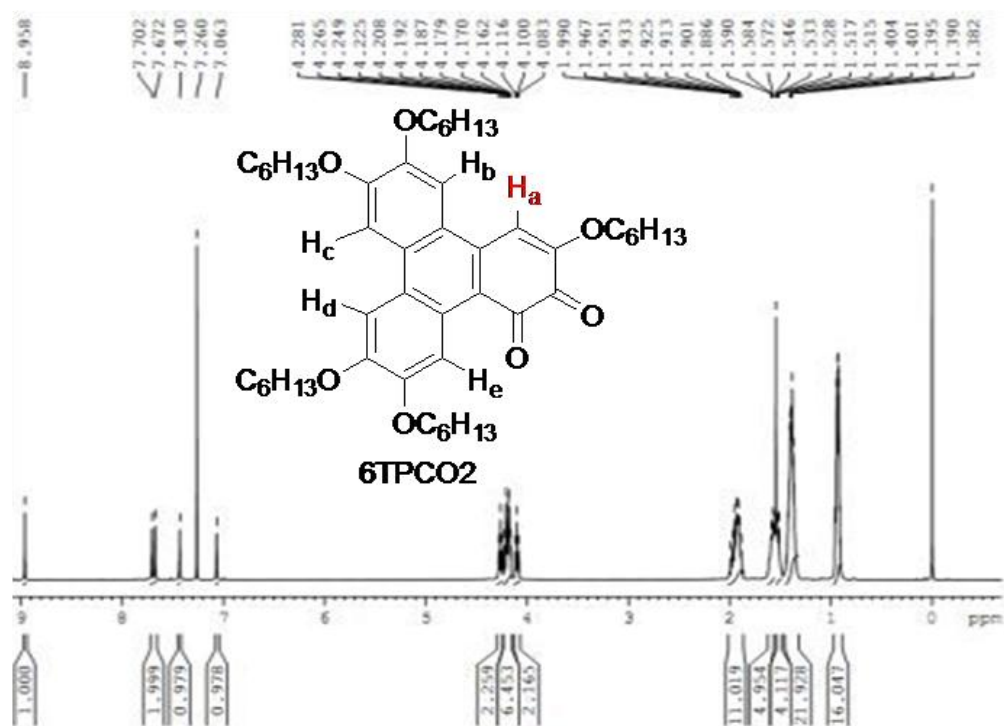
Figure 1. ^{1}H NMR spectrum of the compound **6TPCO2**.

Five different types of protons can be seen at different δ values above δ 7.0 ppm. The resonance peak corresponding to **Ha** appears at δ 8.96 ppm (Structure **6TPCO2**, Figure 1). Other triphenylene protons appear in the range of δ 7.06 to δ 7.70 ppm. Ten ethereal protons of O-**CH₂** group appear as multiplets in between δ 4.05-4.30 ppm. The end methyl protons can be observed at δ 0.93 ppm. Other aliphatic protons of the peripheral alkyl chains can be visibly perceived in the spectrum at δ 1.3-2.0 ppm. ^{1}H NMR spectrum of **6TPIM0** has been represented in Figure 2.
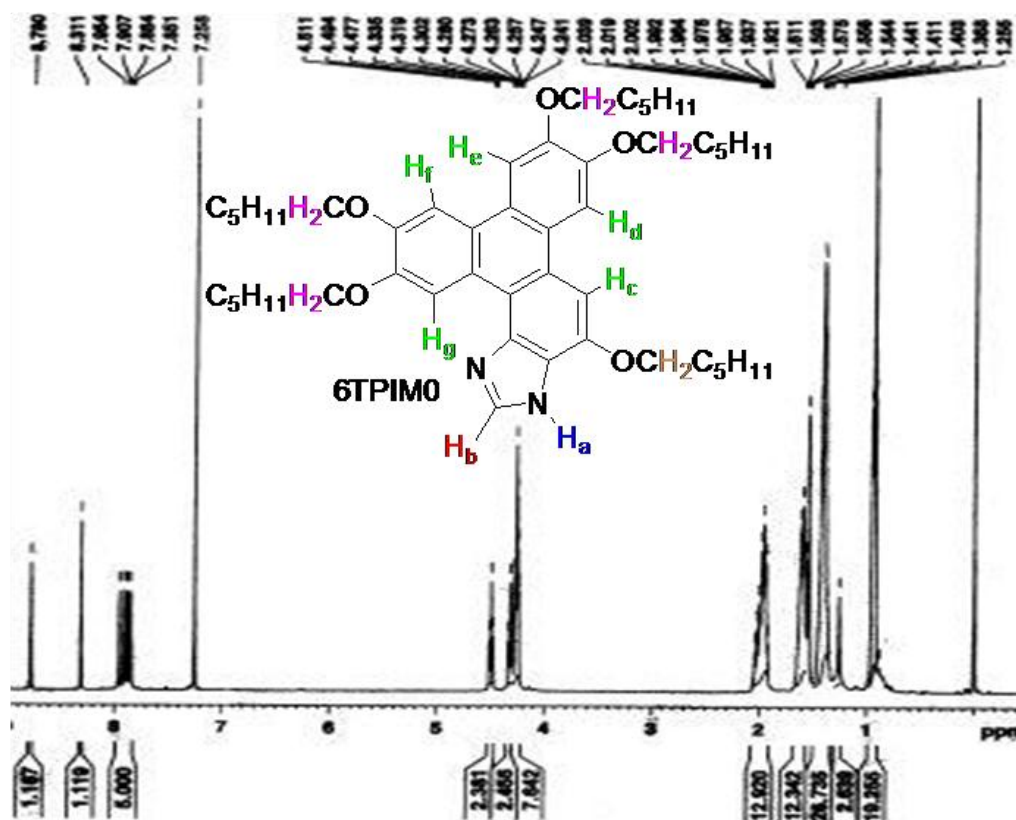
Figure 2. ^{1}H NMR spectrum of the compound **6TPIM0**.

In aromatic region two distinct singlet peaks can be observed at δ 8.78 ppm and δ 8.31 ppm. These peaks correspond to $\mathbf{H_a}$ and $\mathbf{H_b}$ protons, which are attached to imidazole nucleus of **6TPIM0**. The remaining triphenylene protons ($\mathbf{H_c}$, $\mathbf{H_d}$, $\mathbf{H_e}$, $\mathbf{H_f}$, $\mathbf{H_g}$) appear as a cluster of peaks at δ 7.85-7.95 ppm. The –OC$\mathbf{H_2}$ protons of peripheral alkoxy chain adjescent to imidazole ring resonate as triplet at δ 4.49 ppm. The –OC$\mathbf{H_2}$ protons of remaining peripheral alkoxy chains can be visualized as collection of multiplets in between the range of δ 4.24-4.34 ppm. The end methyl protons can be observed at δ 0.94 ppm. Other aliphatic protons of the peripheral alkyl chains can be visibly perceived in the spectrum at δ 1.2-2.1 ppm. Figure 3 is the reproduction of the ^{1}H NMR spectrum of compound **6TPIM6**.
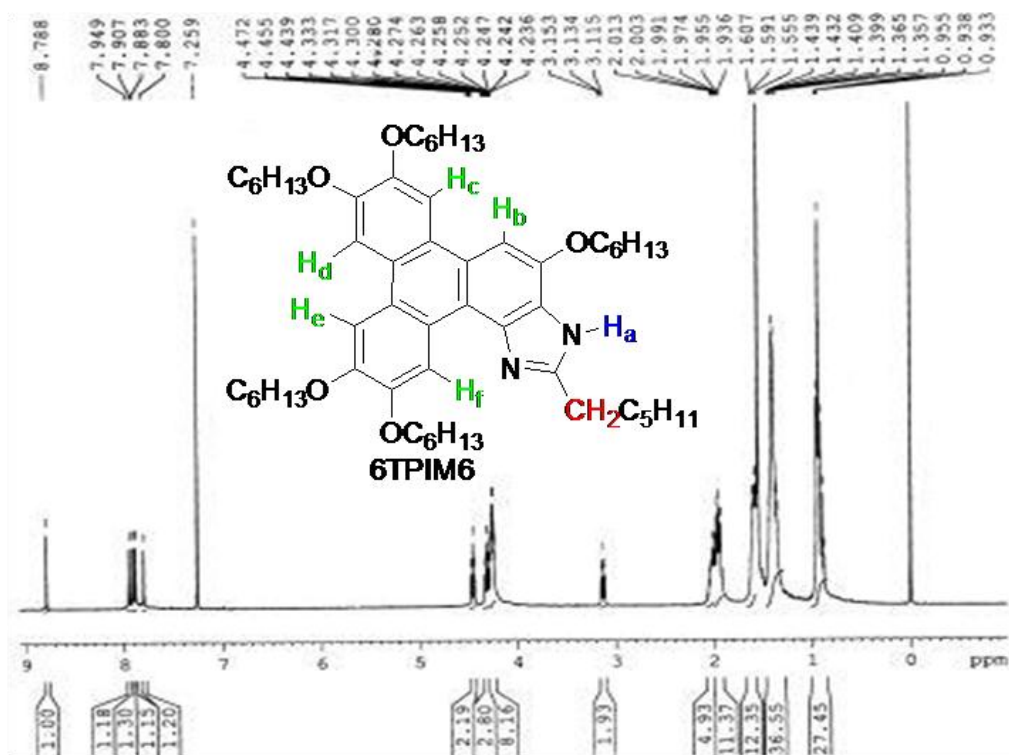
Figure 3. ^{1}H NMR spectrum of the compound **6TPIM6**.

On comparing molecular structure and ^{1}H NMR spectrum of **6TPIM6** with the same of **6TPIM0**, we can see that the peak near δ 8.31 ppm is missing in the spectrum of **6TPIM6**, which is present in the spectrum of **6TPIM0** (Figure 2). This verifies that imidazole proton (**H$_b$** in **6TPIM0** at δ 8.31 ppm) has been replaced by –CH$_2$C$_5$H$_{11}$ group. This fact can again be proved by the presence of triplet peak at δ 3.13 ppm in the spectrum of **6TPIM6**, which is abscent in the same of **6TPIM0**. This triplet peak corresponds to –**CH$_2$**C$_5$H$_{11}$ chain attached to the carbon atom of imidazole nucleus. The remaining triphenylene protons (**H$_b$, H$_c$, H$_d$, H$_e$, H$_f$**) appear as a cluster of peaks at δ 7.80-7.95 ppm. The –OCH$_2$ protons of peripheral alkoxy chain adjescent to imidazole ring resonate as triplet at δ 4.46 ppm. The –OCH$_2$ protons of remaining peripheral alkoxy chains can be seen as collection of multiplets in the range of δ 4.24-4.33 ppm. The end methyl protons can be observed at δ 0.94 ppm. Other aliphatic protons of the peripheral alkyl chains can be visibly perceived in the spectrum at δ 1.36-2.01 ppm.

[211]

5.5. Thermal behavior

The thermal behavior of all the compounds was investigated by polarizing optical microscopy (POM) and differential scanning calorimetry (DSC). The transition temperature and associated enthalpy data obtained from the heating and cooling cycles of DSC or POM are collected in Table 1. The peak temperatures are given in °C and the numbers in parentheses indicate the transition enthalpy (ΔH) in kcal mol^{-1}.

Table 1. Phase transition temperatures (peak, °C) and associated enthalpy changes (kcal mol^{-1}, in parentheses) of triphenylene-imidazole-fused compounds (see Scheme 1 for chemical structures).

| Compound		First heating scan	First cooling scan
6TPIM0	**DSC**	Cr 118.9 (15.86) Col$_h$ 147.3 (0.34) I	I 143.0 (0.34) Col$_h$ 30.6 (9.32) Cr
	POM	Cr 110 Col$_h$ 154 I	I 151 Col$_h$ 51 Cr
6TPIM6	**DSC**	g 108.4 (0.17) Col$_h$ * I	I 140.9 (0.18) Col$_h$
	POM	g 116 Col$_h$ 146 I	I 137 Col$_h$

* Not detected clearly in DSC

5.5.1. Thermal behavior of 6TPIM0:
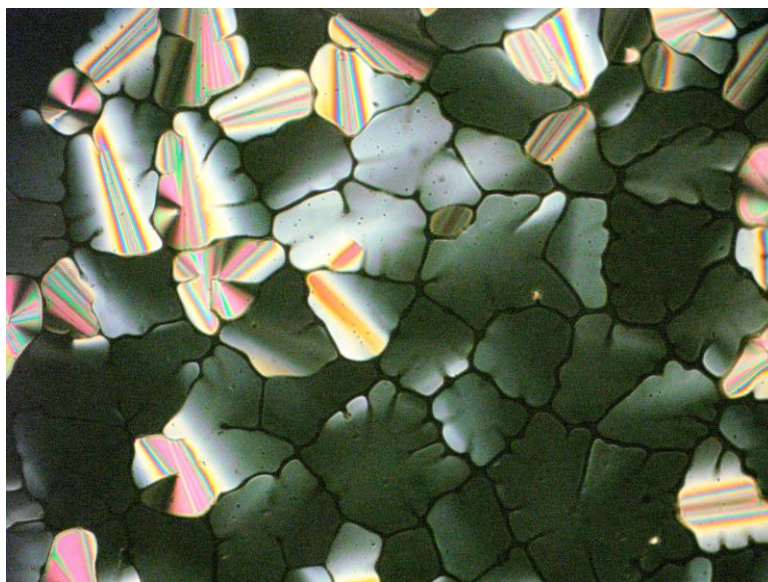
Figure 4. Optical photomicrograph of **6TPIM0** at 138 °C on cooling from the isotropic liquid (crossed polarizers, magnification × 200).

5.5.1.1. **Optical microscopy.** Compound **6TPIM0** was found to be liquid crystalline from 110 °C to 154 °C on heating. On slow cooling from the isotropic liquid, the microscopic preparation revealed a texture which is typical of that of a hexagonal columnar mesophase with large monodomains (Figure 4). On cooling, the crystallisation was confirmed by the slow appearance of small niddle like domains into the liquid crystal texture. It is notable that this transformation occurred at a much lower temperature than the crystal-to-mesophase transformation determined on heating.
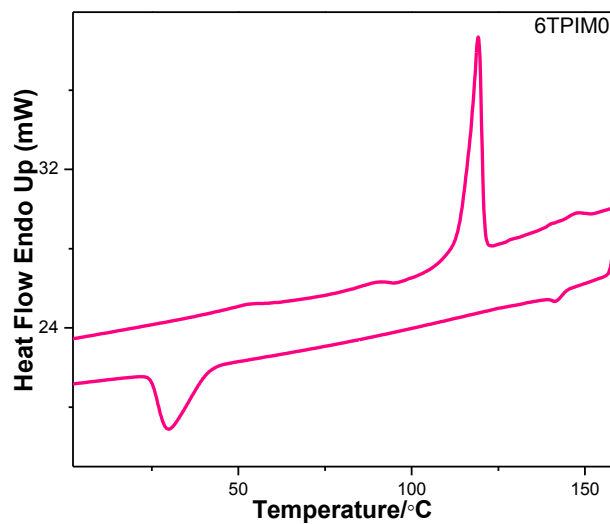
Figure 5. DSC thermogram of **6TPIM0** on heating and cooling cycles (scan rate 10 °C min^{-1}).

5.5.1.2. **DSC.** Two endothermic peaks were observed during the first heating from -30 °C up to 160 °C (Figure 5). The peak at 118.9 °C corresponds to the melting of the crystalline phase into the mesophase, followed by a small one at 147.3 °C, associated to the clearing temperature. On first cooling two exothermic peaks were seen, the first one at 143 °C corresponds to isotropic-to-columnar transition and the second one at 30.6 °C. Further heating and cooling scans of the sample gave almost similar thermal behavior.

5.5.2. Thermal behavior of 6TPIM6:
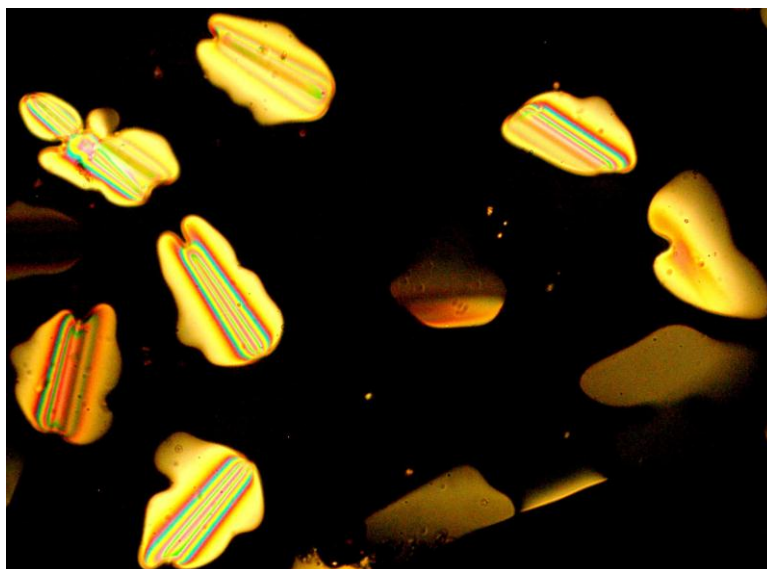
Figure 6. Optical photomicrograph of **6TPIM6** at 130 °C on cooling from the isotropic liquid (crossed polarizers, magnification × 500).

5.5.2.1.   Optical microscopy. POM shows that this compound exhibits enantiotropic mesomorphism. The mosaic-like optical texture is typical for a hexagonal columnar discotic mesophase, normally observed for triphenylene derivatives (Figure 6). No sign of crystallisation or glass formation of the sample could be detected on cooling, and the texture remained unchanged, the mesophase appearing more viscous.

5.5.2.2.   DSC. One endothermic peak corresponding to glass-to-Col_h transformation was observed at 108.4 °C during the first heating from -30 °C up to 160 °C. Unfortunately, no other peak related to Col_h–to-isotropic transition was noticed at higher temperature. However the sample cleared at 146 °C under microscope. On first cooling one exothermic peak was detected, at 140.9 °C corresponding to isotropic-to-columnar transition. No other transition (such as crystallisation or glass transition) was seen down to -30 °C.

OC_6H_{13}
OC_6H_{13}
$C_6H_{13}O$
$C_6H_{13}O$
OC_6H_{13}
HAT6 OC_6H_{13}
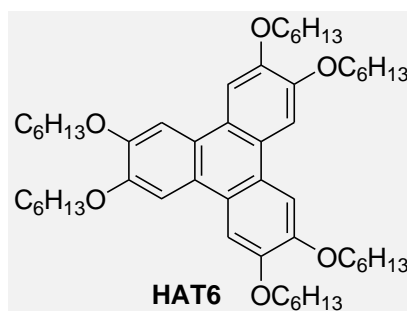
It is prominent that melting as well as isotropization temperature of these compounds is much higher as compared to that reported in case of hexahexyloxytriphenylene (**HAT6**).[26] This behavior can be explained in terms of increased ratio of rigid-to-flexible portions in the mesogen due to extention of triphenylene ring in to triphenylene-imidazole ring without increasing the number or length of peripheral alkyl chains. The compound **6TPIM0** crystallizes at lower temperature, whereas **6TPIM6** remains mesomorphic on cooling. This indicates that attachment of additional flexible hexyl chain to imidazole-fused triphenylene discotic suppresses crystallization and favors liquid crystallinity.

5.6.   X-ray diffraction studies

In order to reveal the mesophase structure and hence the supramolecular organization of these compounds, X-ray diffraction experiments were carried out using unoriented samples. X-ray diffraction patterns for compounds were recorded in the columnar phase around 10 °C below the clearing temperature while cooling from the isotropic phase. The X-ray diffraction patterns of the mesophase exhibited by samples are supportive of a discotic hexagonal columnar arrangement.

---

[26] (a) I. Paraschiv, P. Delforterie, M. Giesbers, M. A. Posthumus, A. T. M. Marcelis, H. Zuilhof, E. J. R. Sudholter, *Liq. Cryst.*, 32, 8, 977, **2005**; (b) P. J. Stackhouse, M. Hird, *Liq. Cryst.*, 35, 5, 597, **2008**.

5.6.1. 6TPIM0

The X-ray diffraction pattern of compound **6TPIM0** and its one dimensional intensity *vs* theta (θ) graph derived from the pattern are shown in the Figure 7.
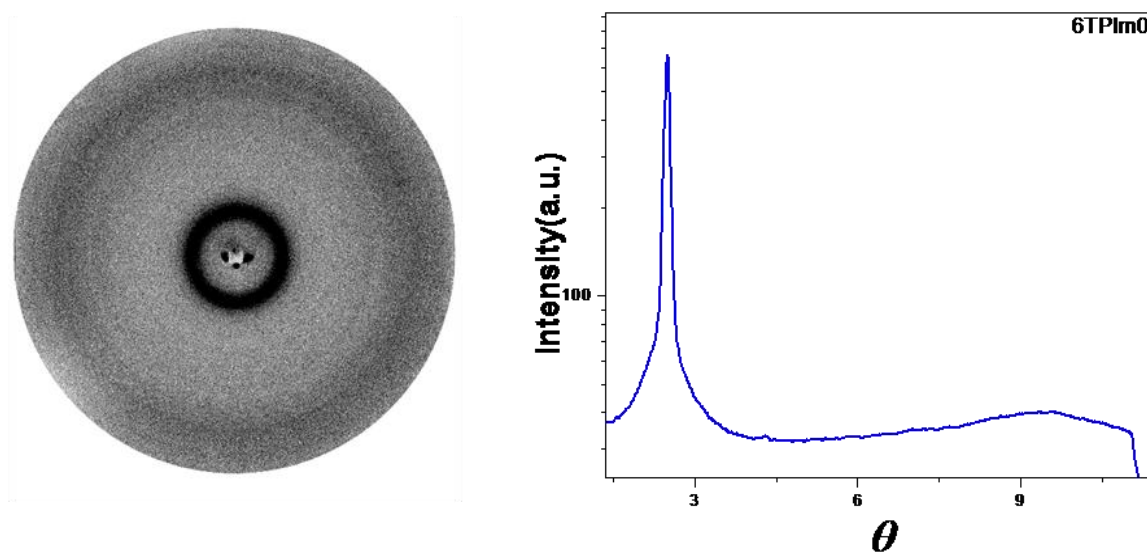
Figure 7. X-ray diffraction pattern and intensity vs θ profile of **6TPIM0** at 130 °C.

In the small angle region, two peaks were observed, one very strong and second weak peak. Taken in the ascending order of diffraction angle, the *d*-spacings of the first reflection (lowest angle and highest intensity) to the second one is in the ratio of 1: $1/\sqrt{3}$. These values correspond to those expected from a two-dimensional hexagonal lattice. In the wide angle region there is one broad peak at $\theta \sim 10^{o}$. This broad peak with a *d*-spacing of ~ 4.7 Å was due to the liquid like packing of the aliphatic chains. The intercolumnar distances, *a*, calculated by using the relation a = $d_{10}/(\cos 30°)$, where d_{10} is the spacing corresponding to the strongest peak in the small angle region, was found to be 20.45 Å. All the features fit into the well known model for the Col_h phase in which the disc-like core of the molecules stack one on top of the other to form columns surrounded by alkyl chains and these columns in turn arrange themselves in a two-dimensional hexagonal lattice. Figure 8 represents X-ray diffraction pattern and one dimensional intensity *vs* theta (θ) graph of compound **6TPIM0** at various temperatures while heating.

[217]
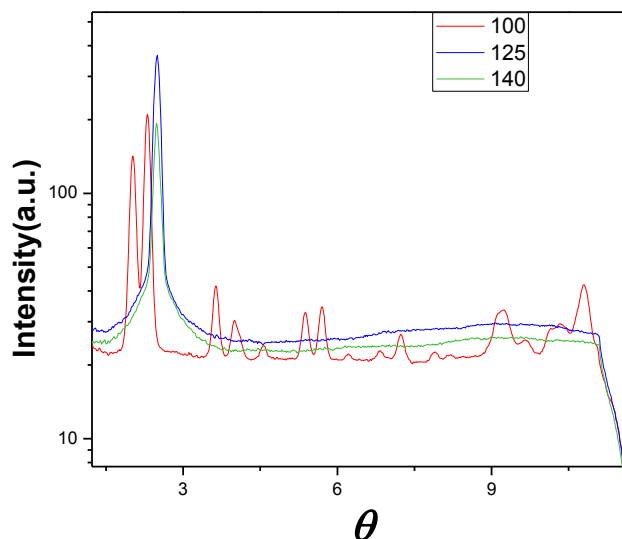
Figure 8. Intensity vs θ profile of **6TPIM0** at 100, 125 and 140 °C while heating.

As may be seen from the figure that the pattern of the compound has numerous sharp peaks in small and wide angle at 100 °C. This indicates that the material is in crystalline phase at this temperature. Whereas at higher temperatures (125 °C, 140 °C) the material exhibited liquid crystalline behavior. This behavior has been proved by DSC and POM.

5.6.2. 6TPIM6

X-ray diffraction pattern and its derived one dimensional intensity versus θ graph of **6TPIM6** are shown in Figure 9.
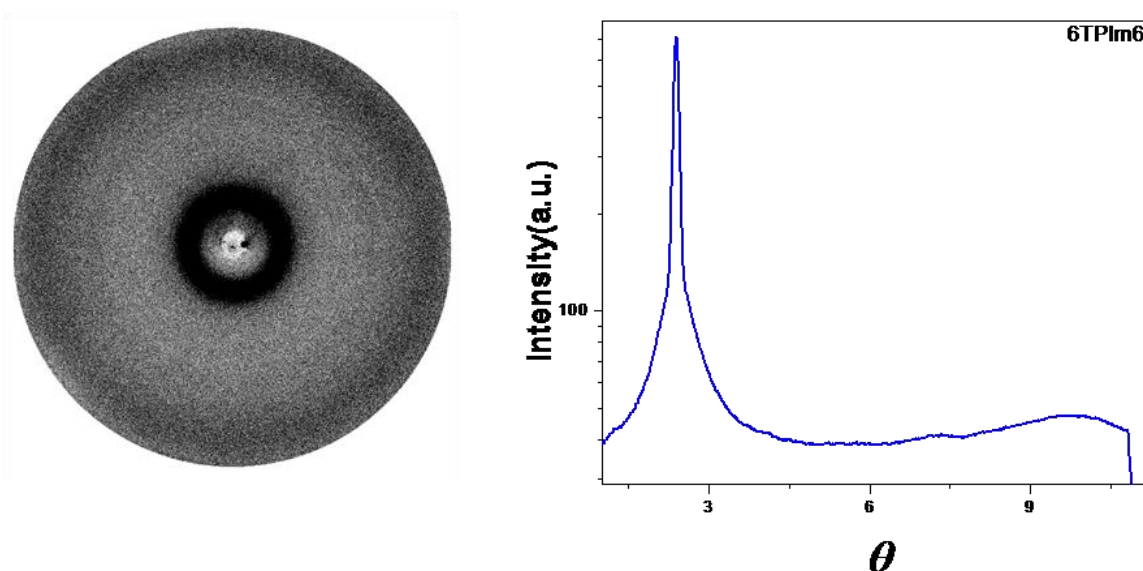
Figure 9. X-ray diffraction pattern and intensity vs θ profile of **6TPIM6** at 125 °C.

As can be seen from the pattern there is one peak at 18.47 Å in small angle region corresponding to (10) reflection from (10) plane of 2D hexagonal columnar lattice. Unfortunately, we did not get any other peak corresponding to higher reflections (11, 20 and so on) in small angle region. The pattern in wide angle region has one broad peak at θ ~ 10°. This broad peak with a *d*-spacing of ~ 4.5 Å was due to the liquid like packing of the aliphatic chains. The intercolumnar distances, *a*, calculated by using the relation a = d_{10}/(cos30°), where d_{10} is the spacing corresponding to the strongest peak in the small angle region, was found to be 21.33 Å.

Table 2. Intercolumnar distances (Å) of **6TPIMx** derived from their diffraction patterns.

Compound	*d*-Spacing (Å)	Intercolumnar distance (Å)
6TPIM0	17.71	20.45
6TPIM6	18.47	21.33
H6TP[26a]	18.34	21.17

It is evident that as number of alkyl chains increases the diameter of the cylindrical columns formed by the discotic molecules also increases. This can be assumed as a reason for higher value of intercolumnar distance of **6TPIM6** as compared to the same observed in case of **6TPIM0** (Table 2). Because of same reason the intercolumnar distance of **6TPIM0** is smaller as compared to that observed for hexahexyloxytriphenylene (**H6TP**). The value of intercolumnar distance is maximum for **6TPIM6** (Table 2). For **6TPIM6**, combined effect of extended discotic core and six peripheral chains (five hexyloxy and one hexyl) plays an important role for the highest value of intercolumnar distance.

5.7. Photoconductivity study

The direct current photo conductivity of pure **6TPIM0** was performed in indium tin oxide (ITO) coated glass sandwich cells (7 mm × 7 mm) with a separation of 4.27 μm. The current measurements were carried out using a Keithley pico ammeter (Model 480) along with a constant voltage source and a temperature controller. Halogen lamp with 20 mW has been used as a source. Resistance Temperature detetector (RTD) is used for measuring resistance with change in temperature of the sample cell. Multimeter is used for resistance measurement.

Dark and photo DC conductivity of **6TPIM0** has been measured in bulb off and bulb on condition with respect to temperature while cooling. Figure 10 illustrates the DC photo and dark conductivity values measured at different temperatures for pure **6TPIM0**, in bulb on and bulb off condition while cooling from isotropic temperature between the range of 160.28-35.99 °C.
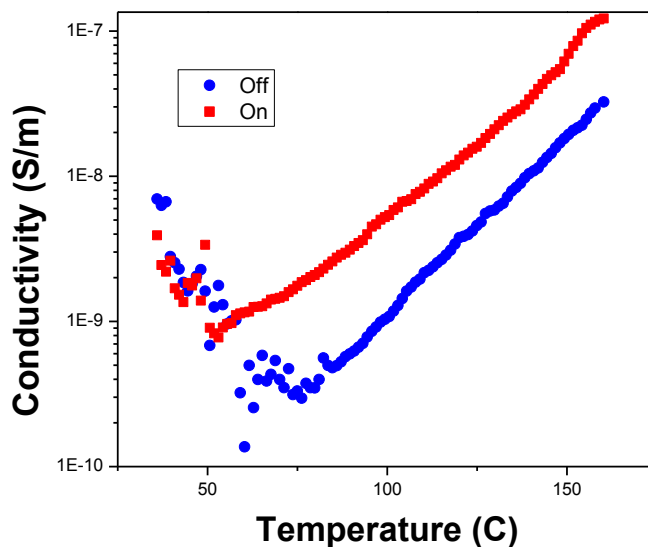
Figure 10: The variation of measured DC photo conductivity values as a function of temperature for **6TPIM0** in bulb on and off condition.

It can be seen that the measured photo conductivity values decrease smoothly between 160.3 °C (1.2 x 10^{-7} S/m) and 53.0 °C (7.7 x 10^{-10} S/m). At lower temperature (below 53.0 °C), there is too much fluctuation in the conductivity value. This temperature is very close to the point (51 °C) where we perceived sign of crystallization during textural observation on cooling from isotropic. On cooling, the maximum and minimum values of measured photoconductivity in mesomorphic range are 4.0x10^{-8} S/m (at 142.0 °C) and 7.7x10^{-10} S/m (at 53.0 °C), respectively. We can compare these photoconductivity values with that of hexahexyloxy triphenylene.[27] The value of measured photoconductivity for hexahexyloxy triphenylene was approximately one order of magnitude lower than current values.

In dark condition, the measured conductivity is lower as compared to the same observed in bulb on condition. There is gradual decrease in the conductivity value between 160.3 °C (3.3 x 10^{-8} S/m) and 84.7 °C (4.8 x 10^{-10} S/m) while cooling. There is too much fluctuation in the measured conductivity value below 84.7 °C. The maximum value of measured DC conductivity in liquid crystalline phase is 1.1x10^{-8} S/m (at 142.0 °C). These DC

---

[27] Kavita, Avinash, S. Kumar, V. LAkshminarayanan; Submitted to *J. Phys. Chem. C.*

conductivity values (bulb off condition) are about one order of magnitude greater as compared to the same measured in case of pure triphenylene-anthraquinone-triphenylene trimer (Chapter 4) and pure hexaheptyloxytriphenylene[28] in their liquid crystalline range. However DC conductivity of this compound is about three orders of magnitude greater than the same obtained in case of hexa(hexylthio)triphenylene.[29] Higher values of photoconductivity and DC conductivity of **6TPIM0** can be explained in terms of extension of triphenylene ring by fusion with imidazole ring. The added imidazole ring enhances π-electron conjugation of triphenylene ring, which can provide better possibility for strong π-π interaction between the polyaromatic cores of resultant disc in the columnar hexagonal phase. Additional stabilization of the columnar mesophase because of increased size of polyaromatic core can be assumed to be the reason for enhanced DC conductivity and photoconductivity, thus making these materials prospective candidates for application in photovoltaic devices.

It is notable that the variation in conductivity with respect to tempetarure does not match with transition temperatures observed while cooling in DSC (Table 1, Figure 5). This can be explained in terms of orientation behavior of discs within the column. Phase transition is a thermodynamic phenomenon, directly related to enthalpy associated with the phase transition. Conductivity, on the other hand is bluntly associated with the degree of orientation of triphenylene discs within the column. In the present case the cooling rate throughout the measurement of conductivity was adjusted to 1.8 °C min^{-1}, which is very low as compared to the scan rate of 10 °C min^{-1} in DSC measurement.

We have also performed photoconductivity experiment for 0.5 % w/w of $HAuCl_4$ in **6TPIM0** in order to examine any effect in photoconductivity after doping. The direct current photo conductivity of this composite was performed in indium tin oxide (ITO) coated glass sandwich cells (7 mm × 7 mm) with a separation of 3.53 µm. Direct current photo conductivity has been measured in bulb on and bulb off condition with respect to temperature while cooling. Figure 11 points up the DC photo conductivity values measured at different temperatures for the composite, in bulb on and bulb off condition while cooling from isotropic temperature between the range of 162.7-35.0 °C.
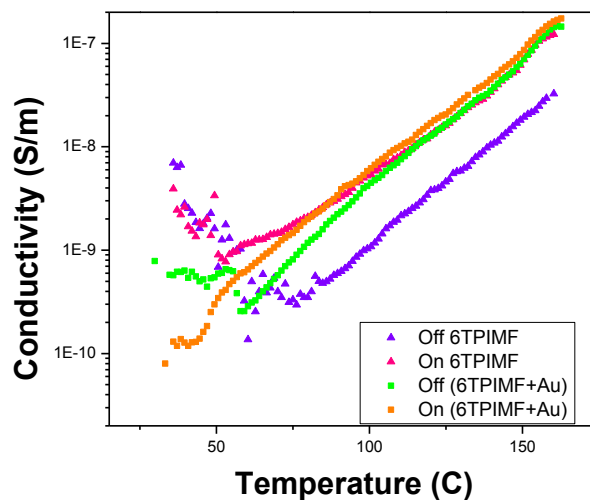
[28] S. Kumar, S. K. Pal, K. P. Suresh, V. Lakshminarayanan, *Soft Matter*, 3, 896, **2007**.
[29] G. B. M. Vaughan, P. A. Heiney, J. P. McCauley Jr, A. B. Smith III, *Phys. Rev b*, 46, 5, 2787, **1992**.
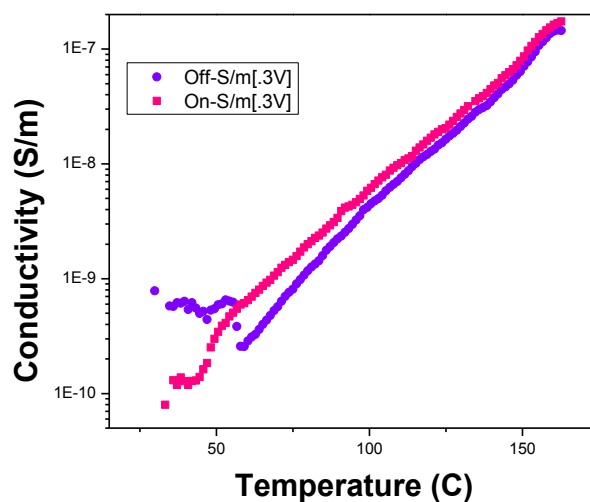
Figure 11: The variation of measured DC photo conductivity values as a function of temperature for 0.5 % w/w HAuCl₄ in **6TPIM0** in bulb on and off condition.

Figure 12: The variation of measured DC photo conductivity values as a function of temperature for **6TPIM0** and 0.5 % w/w HAuCl₄ in **6TPIM0** in bulb on and off condition.

It is clear from the Figure 12 that there is no or very little increment in photoconductivity value after doping the compound. The measured photo conductivity values decrease smoothly between 162.7 °C (1.7 x 10⁻⁷ S/m) and 49.4 °C (3.0 x 10⁻¹⁰ S/m). A change in the slope of the conductivity-temperature plot is observed at 49.4 °C. Microscopic

[223]

experiment reveals the occurance of crystallization at approximately 51 °C on cooling, which is very close to the point (49.4 °C, 3.0 x 10^{-10} S/m) where we are noticing a change in the slope of plot. At lower temperature (below 43.3 °C, 1.3 x 10^{-10} S/m), there is too much fluctuation in the conductivity value. On cooling, the maximum and minimum values of measured photoconductivity in mesomorphic range are 1.3x10^{-7} S/m (at 155.4 °C) and 3.4x10^{-10} S/m (at 50.6 °C), respectively.

In dark condition (bulb off) the value of measured conductivity is found to be slightly lower as compared to the same observed in case of bulb on condition (Figure 11, 12). The measured conductivity values decrease smoothly between 160.3 °C (1.4 x 10^{-7} S/m) and 98.1 °C (4.0 x 10^{-9} S/m). A change in the slope of the conductivity-temperature plot is observed below 98.1 °C. The conductivity value is again decreasing smoothly between 96.9 °C (3.5 x 10^{-9} S/m) to 59.1 °C (2.56 x 10^{-10} S/m). Too much fluctuation in the conductivity value was noticed below 57.9 °C (2.57 x 10^{-10} S/m).

5.8.   Conclusion

The synthesis, characterization and mesomorphic behavior of two novel non-conventional triphenylene derivatives are presented here. One derivative (*i.e.* **6TPIM0**) is having five peripheral hexyloxy chains around the discotic core, while the other one (*i.e.* **6TPIM6**) contains one additional peripheral hexyl chain apart from five hexyloxy chains at the periphery. Liquid crystalline behavior of these two triphenylene-imidazole-fused unsymmetrical derivatives was confirmed by polarizing optical microscopy and differential scanning calorimetry. They exhibit columnar mesophase over a wide range of temperature. Hexagonal columnar structure of the mesophase of these compounds was recognized by X-ray diffraction studies. Addition of one alkyl chain to the periphery of non-conventional triphenylene core (compare **6TPIM6** *vs* **6TPIM0**) results in expansion of hexagonal columnar lattice. We observed reasonable increment in mesophase range and improvement in DC electrical and DC photoconductivity after fusion of triphenylene ring with imidazole nucleus.

5.9. Experimental

5.9.1. General information

General experimental conditions have been described in chapter 2.

5.9.2. General procedure for the synthesis of 6TPCO2

Ammonium ceric nitrate (405 mg, 0.739 mmol) was added to a stirred solution of monohydroxytriphenylene (500 mg, 0.671 mmol) in acetonitrile at room temperature. The reaction mixture was stirred at room temperature for about three minutes. The product was separated from the solvent by normal filtration. The residue was purified by column chromatography over silica gel (eluant: 10 % ethyl acetate in hexane) to yield **6TPCO2** as a dark blue coloured solid (332.8 mg, 65.33 %).

^{1}H NMR (400 MHz, CDCl$_3$): δ 8.96 (s, 1H), 7.67 (d, 2H), 7.43 (s, 1H), 7.06 (s, 1H), 4.21 (m, 10H), 1.93 (m, 10H), 1.3-1.6 (m, 30H), 0.93 (m, 15H).

UV-Vis data (CHCl$_3$): λ_{max} 271, 339, 383, 561 nm.

5.9.3. Synthesis of 6TPIMx: General Procedure.

In a reaction, a stirred mixture of **6TPCO2** (332.8 mg, 0.438 mmol), formaldehyde (0.0711 ml, 37 wt %), glacial acetic acid (2 ml) and ammonium acetate (701.7 mg, 9.1 mmol) was refluxed for 4.5 hours. After cooling the reaction mixture was diluted with water. Concentrated aqueous ammonia solution (sp. gr 0.91, 25-28 wt %) was added to neutralize the solution up to pH 7. A brown precipitate was formed. It was filtered, washed with distilled water. The residue was extracted with a mixture of chloroform and distilled water. The organic extract was dried over anhydrous sodium sulphate, concentrated and the product was purified by repeated column chromatography over silica gel (eluant: 5% ethyl acetate in hexane). Solvent was then removed in rotary evaporator. The residue left was now dissolved in dichloromethane and the resulting solution was added to cold methanol to afford **6TPIM0**

as gray color solid (90 mg, 26.69 %). Simillarily, **6TPIM6** was obtained as dark brown sticky material in 28.36 % yield.

6TPIM0

¹H NMR (400 MHz, CDCl$_3$): δ 8.78 (s, 1H), 8.31 (s, 1H), 7.8-8.0 (m, 5H), 4.49 (t, J = 6.6, 2H), 4.32 (t, J = 6.6, 2H), 4.26 (m, 6H), 1.96 (m, 10H), 1.2-1.7 (m, 30H), 0.94 (m, 15H).

UV-Vis data (CHCl$_3$): λ$_{max}$ 282, 353, 371 nm.

Elemental analysis: Calcd for C$_{49}$H$_{72}$N$_2$O$_5$, C 76.52, H 9.44, N 3.64; Found C 76.63, H 9.64, N 3.69%.

HRMS (Methanol+Chloroform, m/z): 769.55 (M)$^+$, 770.55 (M+H)$^+$, 771.56 (M+2H)$^+$, 647.41, 643.38, 615.36, 409.19, 361.12, 306.19, 305.19, 187.13, 131.06.

6TPIM6

¹H NMR (400 MHz, CDCl$_3$): δ 8.79 (s, 1H), 7.8-7.9 (m, 5H), 4.46 (t, J = 6.8, 2H), 4.32 (t, J = 6.7, 2H), 4.26 (m, 6H), 3.13 (t, J = 7.8, 2H), 1.96 (m, 10H), 1.2-1.7 (m, 38H), 0.94 (m, 18H).

UV-Vis data (CHCl$_3$): λ$_{max}$ 283, 351, 369 nm.

Elemental analysis: Calcd for C$_{55}$H$_{84}$N$_2$O$_5$, C 77.42, H 9.92, N 3.28; Found C 77.03, H 10.17, N 3.06%.